Inorganic Chemistry

Article

pubs.acs.org/IC

Formation of New Non-oxido Vanadium(IV) Species in Aqueous Solution and in the Solid State by Tridentate (O, N, O) Ligands and Rationalization of Their EPR Behavior

Daniele Sanna,[†] Katalin Várnagy,[‡] Norbert Lihi,[‡] Giovanni Micera,[§] and Eugenio Garribba*[,§]

[†]Istituto CNR di Chimica Biomolecolare, Trav. La Crucca 3, I-07040 Sassari, Italy

[‡]Department of Inorganic and Analytical Chemistry, University of Debrecen, H-4010 Debrecen, Hungary

[§]Dipartimento di Chimica e Farmacia and Centro Interdisciplinare per lo Sviluppo della Ricerca Biotecnologica e per lo Studio della Biodiversità della Sardegna, Università di Sassari, Via Vienna 2, I-07100 Sassari, Italy

Supporting Information

ABSTRACT: The systems formed by the $V^{IV}O^{2+}$ ion with tridentate ligands provided with the (O, N_{imine}, O) donor set were described. The ligands studied were 2,2′-dihydroxyazobenzene (Hdhab), α-(2-hydroxy-5-methylphenylimino)-*o*-cresol (Hhmpic), calmagite (H_2calm), anthracene chrome red A (H_3anth), calcon (H_2calc), and calconcarboxylic acid (H_3calc^C). They can bind vanadium with the two deprotonated phenol groups and the imine nitrogen to give (5,6)-membered chelate rings. The systems were studied with EPR, UV−vis and IR spectroscopy, pH-potentiometry, and DFT methods. The ligands form unusual non-oxido V^{IV} compounds both in aqueous solution and in the solid state. $[V(anthH_{-1})_2]^{4-}$ and $[V(calmH_{-1})_2]^{2-}$ (formed in water at the physiological pH) and $[V(dhabH_{-1})_2]$ and $[V(hmpicH_{-1})_2]$ (formed in the solid state in MeOH) are hexa-coordinated with geometry intermediate between the octahedron and the trigonal prism and an *unsymmetric facial* arrangement of the two ligand molecules. DFT calculations were used to predict the structure and ^{51}V hyperfine coupling tensor **A** of the non-oxido species. The EPR behavior of 13 non-oxido V^{IV} species was put into relationship with the relevant geometrical parameters and was rationalized in terms of the spin density on the d_{xy} orbital. Depending on the geometric isomer formed (*meridional* or *facial*), d_{z^2} mixes with the d_{xy} orbital, and this effect causes the lowering of the highest ^{51}V *A* value.

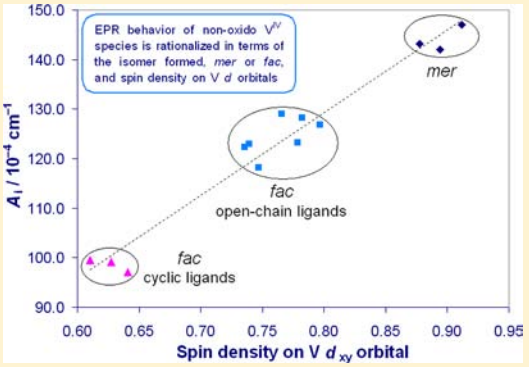

INTRODUCTION

Vanadium is an important trace element for different organisms.[1] Among others, it is present in vanadium dependent haloperoxidases[2] and in nitrogenases[3] and is accumulated in concentrations up to 0.3 M in the vanadocytes of ascidians and polychaete worms.[4] Vanadium also has an important role in the human organism, and it is probably involved in the regulation of phosphate metabolism.[5] As from 1980, it has been demonstrated that many vanadium compounds have therapeutic effects as insulin-enhancing agents,[6,7] whose transport in the blood has been recently investigated.[8,9]

The only oxidation states relevant for biological systems are III, IV, and V.[1,5] In particular, it has been suggested that, almost independently of the initial state, about 90% of the vanadium present in the blood is associated with the plasma fraction in the $V^{IV}O^{2+}$ form.[9d,10] The binding of $V^{IV}O^{2+}$ to bioligands such as GSH, NADH, and ascorbate can further stabilize the IV state and prevent its oxidation to vanadium(V).[11]

The chemistry of vanadium(IV) is dominated by the $V^{IV}O^{2+}$ ion. The formation of non-oxido or "bare" hexa-coordinated vanadium(IV) complexes is rather difficult because the strong V═O bond must be broken, and the oxido ligand leaves the complex as a water molecule. The number of non-oxido vanadium(IV) complexes found within the Cambridge Structural Database[12] still remains relatively scarce and is much lower than that of oxidovanadium(IV) species. However, non-oxido vanadium centers have important biological functions and have been reported for amavadin, a complex isolated by Bayer and Kneifel from *Amanita muscaria*[13] and characterized by Garner and co-workers,[14] and for the cofactor of vanadium nitrogenase.[3] This has stimulated over the past few years the synthesis and investigation of new non-oxido vanadium(IV) complexes. In 2007, new models of amavadin were synthesized with tetradentate ligands.[15] Up to date, non-oxido V(IV) structures with VO_3S_3,[16] VO_6,[17] VS_6,[18] VO_4N_2,[19] and VO_4X_2 (X = S, Se, P)[20] coordination have been reported. The formation of these "bare" species is significantly favored by the preorganization of the tridentate ligand, as in the case of *cis*-inositol derivatives.[21]

Depending on the specific ligand, several geometries (octahedral and trigonal prismatic),[22] ground states (d_{xy} or

Received: April 30, 2013
Published: July 2, 2013

   dx.doi.org/10.1021/ic401080q | *Inorg. Chem.* 2013, 52, 8202−8213

d_{z^2}),[23] isomers (*facial* or *meridional* when the ligand is tridentate),[19c,20] and spectroscopic responses (EPR and UV−vis)[24] are possible. Hexa-coordinate non-oxido vanadium(IV) complexes exhibit a geometry intermediate between the octahedron and trigonal prism. With ligands forming a five-membered chelate ring such as *o*-catechols, *o*-mercaptophenols, and dithiolenes, the geometry is close to the trigonal prism, and there is a switch of the ground state from d_{xy} to d_{z^2}.[25] The distortion degree of the octahedron can be expressed by the twist angle Φ between the triangular faces of the coordination polyhedron (Φ is 60° for a regular octahedron and 0° for a trigonal prism). The transformation of an oxido into a non-oxido vanadium(IV) species can be followed by EPR spectroscopy; in particular, a significant decrease of the isotropic (A_{iso}) and anisotropic (A_i, with $i = x, y, z$) ^{51}V hyperfine coupling constant, from 80−105 (A_{iso} for $V^{IV}O$ complexes) and 150−180 × 10^{-4} cm^{-1} (A_z for $V^{IV}O$ complexes) to 50−75 (A_{iso} for V^{IV} complexes) and 100−140 × 10^{-4} cm^{-1} (A_i with i = *x*, *y*, *z* for V^{IV} complexes), respectively, is observed.[24b]

In this study, the behavior in aqueous solution and in the solid state of the systems containing the $V^{IV}O^{2+}$ ion and ligands potentially able to form non-oxido species was examined. The ligands studied were 2,2′-dihydroxyazobenzene (Hdhab), *α*-(2-hydroxy-5-methylphenylimino)-*o*-cresol (Hhmpic), 3-hydroxy-4-[(2-hydroxy-5-methylphenyl)azo]-1-naphthalenesulfonic acid or calmagite (H_2calm), 3-hydroxy-4-[(2,4-dihydroxy-1-phenyl)-azo]-benzenesulfonic acid or anthracene chrome red A (H_3anth), 3-hydroxy-4-[(2-hydroxy-1-naphthyl)azo]-1-naphthalenesulfonic acid or calcon (H_2calc), and 3-hydroxy-4-[(2-hydroxy-4-sulfo-1-naphthyl)azo]-1-naphthalene-2-carboxylic acid or calconcarboxylic acid (H_3calc^C). These are provided with a (O^-, N_{imine}, O^-) donor set and can form a five- plus a six-membered chelate ring (Scheme 1). Calmagite, anthracene chrome red A, calcon, and calconcarboxylic acid are commonly used as indicators in the complexometric titrations. The difference in their complexation scheme will be discussed in the text.

The study was carried out with the combined application of spectroscopic (EPR, UV−vis, and IR), analytical (pH-potentiometry), and computational (DFT methods) techniques. The results will aid in understanding the structural factors that determine the geometry of the non-oxido V^{IV} complexes as well as in the characterization of the naturally occurring V^{IV} compound, such as amavadin. In particular, ^{51}V hyperfine coupling constants measured in the EPR spectra can be put in relationship with the geometry of hexa-coordinated species and the electronic structure. The stability constants of the V compounds could be used for the possible application of these ligands as chelating indicators in the analytical determination of vanadium.

Scheme 1. Ligands (Donor Atoms Are Represented in Red)

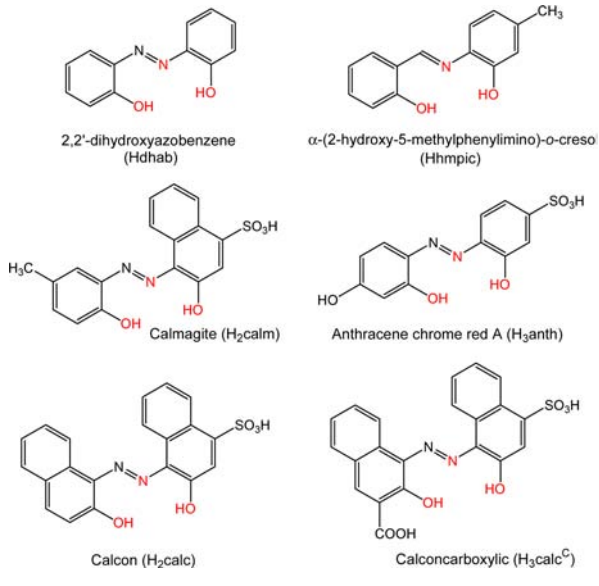

EXPERIMENTAL AND COMPUTATIONAL SECTION

Chemicals. Water was deionized prior to use through the purification system Millipore Milli-Q Academic. $V^{IV}O^{2+}$ solutions were prepared from $VOSO_4{\cdot}3H_2O$ following literature methods.[26] All the ligands were Aldrich or Fluka products of puriss. quality and were used as received.

Potentiometric Measurements. The stability constants of proton and $V^{IV}O^{2+}$ complexes were determined by pH-potentiometric titrations of 3−4 mL of samples. The ligand to metal molar ratio was between 1:1 and 10:1, and the $V^{IV}O^{2+}$ concentration was 4.0 × 10^{-4} to 4.0 × 10^{-3} M. Titrations were performed from pH 2.0 until precipitation or very extensive hydrolysis by adding carbonate-free KOH of a known concentration (ca. 0.2 M KOH).[27] The pH was measured with a Metrohm 6.0234.110 combined electrode, calibrated for hydrogen ion concentration by the method of Irving et al.[28] Measurements were carried out at 25.0 ± 0.1 °C and at a constant ionic strength of 0.2 M KCl with a MOLSPIN pH-meter and a MOL-ACS microburet (0.50 mL) controlled by computer. Purified argon was bubbled through the samples to ensure the absence of oxygen. The number of experimental points was 50−70 for each titration curve, and the reproducibility of the points included in the evaluation was within 0.005 pH unit in the measured pH range. The stability of the complexes, reported as the logarithm of the overall formation constant $\beta_{pqr} = [(VO)_pL_qH_r]/[VO]^p[L]^q[H]^r$, where VO stands for the $V^{IV}O^{2+}$ ion, L is the deprotonated form of the ligand, and H is the proton, has been calculated with the aid of the SUPERQUAD[29] and HYPERQUAD[30] programs. Standard deviations were based on random errors. The conventional notation has been used: negative indices for protons indicate hydroxido ligands or the dissociation of groups which do not deprotonate in the absence of $V^{IV}O$ coordination. Hydroxido complexes of $V^{IV}O^{2+}$ were taken into account, and the following species were assumed: $[VO(OH)]^+$ (log β_{10-1} = −5.94), $[(VO)_2(OH)_2]^{2+}$ (log β_{20-2} = −6.95), with stability constants calculated from the data of Henry et al.[31] and corrected for the different ionic strengths by use of the Davies equation,[32] $[VO(OH)_3]^-$ (log β_{10-3} = −18.0), and $[(VO)_2(OH)_5]^-$ (log β_{20-5} = −22.0).[33] The standard deviations of the stability constants are given in parentheses in Table 1.

For the determination of the stability constants by spectrophotometry, UV−vis spectra of $V^{IV}O/V^{IV}$ complexes were recorded on a Perkin-Elmer Lambda 25 double beam spectrometer in the same concentration range as used for pH-potentiometry. The calculations were performed by means of the PSEQUAD program.[34]

Synthesis of Non-oxido Vanadium(IV) Complexes. $[V(dhabH_{-1})_2]$ and $[V(hmpicH_{-1})_2]$ were synthesized following the procedure established by Chaudhuri and co-workers.[19c] A total of 2.0 × 10^{-4} mol of $VCl_3(THF)_3$ and 4.0 × 10^{-4} mol of ligands were dissolved in the minimum amount of MeOH. Subsequently, Et_3N (0.5 mL) was added, and the resulting solution was refluxed under argon for 30 min. After cooling to room temperature, the solution was opened to air and stirred for 5 min to favor the oxidation of V(III) to V(IV). The solution was then concentrated by passing argon over the surface of the solution to yield a dark crystalline solid. $[V(dhabH_{-1})_2]{\cdot}CH_3OH$. Anal. Calcd for $C_{25}H_{20}N_4O_5V$ (507.40): C, 59.18; H, 3.97; N, 11.04. Found: C, 59.51; H, 3.81; N, 11.10.

dx.doi.org/10.1021/ic401080q | Inorg. Chem. 2013, 52, 8202−8213

Table 1. pK_a Values of the Ligands[a]

	H_3anth	H_2calm			H_2calc		H_3calc^C	
	pot.[b]	pot.[b]	spectr.[b]	literature	spectr.[b]	literature	spectr.[b]	literature
pK_a(OH)$_1$	7.58(1)	8.24(7)	8.05(1)	7.74−8.14[c]	7.73(1)	7.01−8.29[d]	9.74(1)	7.60[e]
pK_a(OH)$_{resor}$	6.35(1)							
pK_a(SO_3H)	<1	<1	<1		<1		<1	
pK_a(COOH)							3.97(4)	4.39[e]

[a]The standard deviations are given between parentheses. [b]Pot. and Spectr. indicate that the values were determined with potentiometry and spectrophotometry, respectively. [c]Ref 47. [d]Ref 48. [e]Ref 49 (value measured in H_2O/MeOH 75:25 v/v).

[V(hmpicH$_{-1}$)$_2$]. Anal. Calcd for $C_{28}H_{22}N_2O_4V$ (501.43): C, 67.07; H, 4.42; N, 5.59. Found: C, 66.84; H, 4.45; N, 5.32.

Spectroscopic Measurements. Anisotropic EPR spectra were recorded on aqueous solutions with an X-band (9.15 GHz) Varian E-9 spectrometer at 100 K. As usual for low temperature measurements, a few drops of DMSO were added to the samples to ensure good glass formation. All operations were performed under a purified argon atmosphere in order to avoid oxidation of the $V^{IV}O^{2+}$ ion. The spectra were simulated with the software Bruker WinEPR SimFonia,[35] using the highest symmetry molecular axis as the z direction: for the $V^{IV}O^{2+}$ species, this coincides with the V═O bond, whereas for the non-oxido V^{IV} complexes with the O−V−O direction. Electronic spectra were recorded with a Perkin-Elmer Lambda 35 spectrophotometer in the same concentration range as used for potentiometry.

Infrared spectra (4000−600 cm^{-1}) were obtained with a Jasco FT/IR-480Plus spectrometer using KBr disks. Elemental analysis (C, H, N) was carried out with a Perkin-Elmer 240 B elemental analyzer.

DFT Calculations. All the geometries of $V^{IV}O$ and V^{IV} complexes were optimized in the gas phase with Gaussian 09 (revision C.01) software,[36] using the hybrid exchange-correlation functional B3P86,[37] and the basis set 6-311g.[38] The functional B3P86 ensures a good degree of accuracy in the prediction of the structures of first-row transition metal complexes,[39] and in particular of vanadium compounds.[40]

The ^{51}V $\boldsymbol{A}$ tensor was calculated using the functional PBE0[41] and VTZ basis set with the ORCA software,[42] according to the procedures published in the literature.[43] The theory background was described in detail in ref 43c.

The spin density on V d orbitals was calculated at the PBE0/VTZ level of theory using a coordinate system in which the z axis is roughly oriented along the two V−O bonds and the x and y axes along the O−V−N directions.

The relative energy of non-oxido V^{IV} species formed in MeOH by Hdhab and Hhmpic was calculated at the B3P86/6-311g level of theory computing the solvent effect with the PCM[44] or SMD[45] model, both available in the Gaussian 09 software. The performances of PCM were well established in the literature.[43e,h,46] The SMD has been recently proposed and is based on the quantum mechanical charge density of a solute molecule interacting with a continuum description of the solvent, which takes into account the full solute electron density without defining partial atomic charges and represents the solvent not explicitly but rather as a dielectric medium with surface tension at the solute−solvent boundary. It has been demonstrated that it gives good results in the prediction of the solvation free energy.[45] The total value of the free energy in solution (ΔG^{tot}_{sol}) can be separated into the electronic plus nuclear repulsion energy (ΔE^{ele}), the thermal contribution (ΔG^{therm}), and the solvation free energy ($\Delta(\Delta G^{solv})$): $\Delta G^{tot}_{sol} = \Delta E^{ele} + \Delta G^{therm} + \Delta(\Delta G^{solv})$. The thermal contribution was estimated using the ideal gas model and the calculated harmonic vibrational frequencies to determine the correction due to zero point energy and to thermal population of the vibrational levels.[46b]

RESULTS AND DISCUSSION

1. Studies in Aqueous Solution. Among the six ligands examined, 2,2′-dihydroxyazobenzene (Hdhab) and α-(2-hydroxy-5-methylphenylimino)-*o*-cresol (Hhmpic) are not soluble in water. Due to the presence of the sulfonic group (and the carboxylic one in case of H_3calc^C), the other four ligands are moderately soluble, even if the potentiometric measurements can be carried out only in diluted solutions (∼ 8.0×10^{-4} M). For this reason, a precise determination of protonation constants was not possible by means of pH-titrations, as can be seen in Table 1. On the other hand, the color of the ligands changes with increasing of the pH, and the protonation constant of calmagite (H_2calm), calcon (H_2calc), and calconcarboxylic acid (H_3calc^C) can be calculated from spectrophotometric data by means of the PSEQUAD program. The pK_a values are summarized in Table 1.

For all the ligands, the deprotonation of the sulfonic group takes place with a pK_a < 1 and cannot be determined.

In the case of anthracene chrome red A, two pK_a values fall into the measurable pH range. For the precise assigning of the deprotonation steps, the calculation of microconstants is needed. One of them belongs to one internal phenolic −OH group and the other to the deprotonation of the "resorcinol" −OH. On the basis of comparison of the pK_a values with those of other ligands, the lower value is assigned to the deprotonation of "resorcinol" −OH.

In the case of calcon and calconcarboxylic acid, there is a significant difference between the pK_a values of the two −OH groups. Furthermore, the deprotonation of the first phenolic group of calconcarboxylic acid takes place at pH much higher than calcon. This effect is due to the deprotonation of the carboxylic group and the formation of a hydrogen bond between carboxylate and the −OH group.

The stability constants of the $V^{IV}O^{2+}$ complexes are summarized in Table 2. Only for anthracene chrome red A is it possible to carry out potentiometric measurements; for the other three systems, because of the scarce solubility of the

Table 2. Stability Constants (log β_{pqr}) of the $V^{IV}O^{2+}$ Complexes at 25.0 ± 0.1 °C and I = 0.20 M (KCl)[a]

	H_3anth	H_2calm	H_2calc	H_3calc^C
	pot.	spectr.	spectr.	spectr.
VOL	13.93(40)			12.12(6)
VOL_2H	24.66(67)			
VOL_2	18.76(46)	18.92(4)		
$VOLH_{-1}$		6.95(3)	8.47(6)	7.66(8)
VOL_2H_{-1}		12.39(2)	12.48(13)	12.33(9)
fitting parameter[b]	0.0034	0.0075	0.029	0.0084
number of fitted data points	131			
number of fitted spectra		14	15	12

[a]The standard deviations are given between parentheses. [b]Fitting parameter is the average difference between the calculated and experimental absorption curves (spectrophotometry) or titration curves expressed in mL of the titrant (potentiometry).

dx.doi.org/10.1021/ic401080q | Inorg. Chem. 2013, 52, 8202−8213

ligands, the stability of the metal complexes was determined through the PSEQUAD program by spectrophotometric titrations. The species distribution diagrams as a function of pH for the systems $V^{IV}O^{2+}/H_3$anth and $V^{IV}O^{2+}/H_3calc^C$ are shown in Figures 1 and 2.

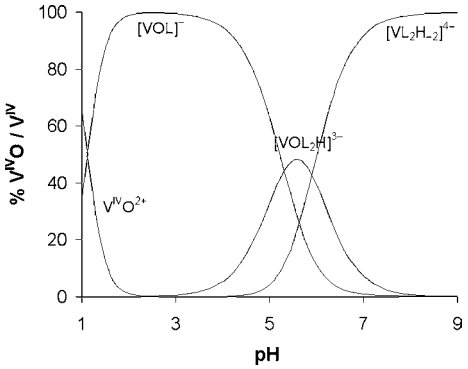

Figure 1. Distribution diagram as a function of pH of the species formed in the system $V^{IV}O^{2+}/H_3$anth (H_3L) with a total $V^{IV}O^{2+}$ concentration of 1.0×10^{-3} M and ligand to metal molar ratio of 10:1.

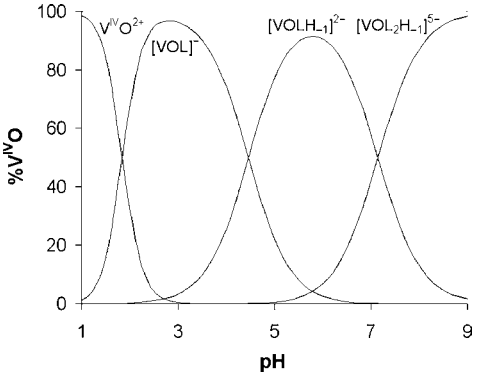

Figure 2. Distribution diagram as a function of pH of the species formed in the system $V^{IV}O^{2+}/H_3calc^C$ (H_3L) with a total $V^{IV}O^{2+}$ concentration of 1.0×10^{-3} M and ligand to metal molar ratio of 10:1.

EPR spectroscopy allowed us to confirm these results. The ligands can be divided into two classes on the basis of their complexing behavior: H_3anth and H_2calm on one hand and H_3calc^C and H_2calc on the other. For simplicity, we will discuss the results of the $V^{IV}O^{2+}/H_3$anth and $V^{IV}O^{2+}/H_3calc^C$ systems as examples of the two classes. EPR spectra recorded as a function of pH for these two systems are shown in Figures 3 and 5, and EPR parameters are collected in Table 3.

In the system $V^{IV}O^{2+}/H_3$anth, at acidic pH values, the VOL species is formed (**I** in Figure 3), which is the main in solution in the pH range 2.0−5.0. The metal ion is able to promote the deprotonation and coordination of both the phenolic groups, whereas the "resorcinol" remains still protonated (VOL = $VO(LH_{-1})H$). We assign to VOL the coordination mode [(O^-, N_{imine}, O^-); H_2O]. The value of A_z is 164.9×10^{-4} cm^{-1}. The additivity rule[50] predicts for this coordination 165.0×10^{-4} cm^{-1}, in good agreement with what is experimentally observed. Interestingly, A_z is comparable with that measured for other tridentate ligands (4-[3,5-bis(2-hydroxyphenyl)-1*H*-1,2,4-triazol-1-yl]benzoic acid (H_3hyph^C), 4-[3,5-bis(2-hydroxyphenyl)-1*H*-1,2,4-triazol-1-yl]sulfonic acid (H_3hyph^S), and 2,6-bis-(2-hydroxyphenyl)pyridine (H_2bhpp)), which form analogous

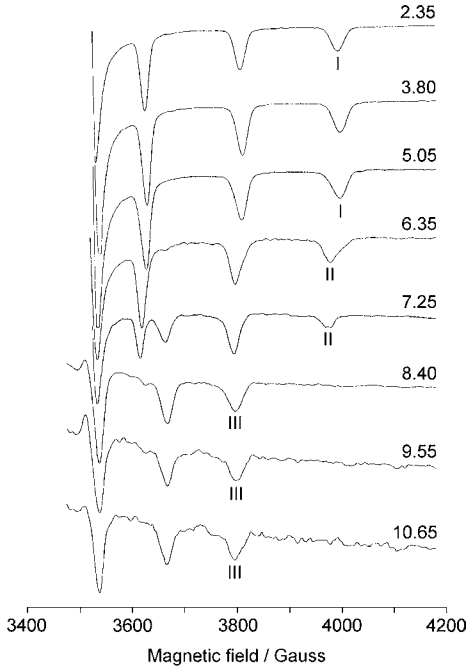

Figure 3. High field region of the X-band anisotropic EPR spectra recorded as a function of pH in the system $V^{IV}O^{2+}/H_3$anth (H_3L) with a total $V^{IV}O^{2+}$ concentration of 4.0×10^{-3} M and ligand to metal molar ratio of 10:1. **I**, **II**, and **III** indicate the $M_I = 7/2$ resonances of $[VOL]^-$, $[VOL_2H]^{3-}$, and $[VL_2H_{-2}]^{4-}$, respectively.

Table 3. EPR Parameters of the $V^{IV}O$ and V^{IV} Complexes Formed in the Systems $V^{IV}O^{2+}/H_3$anth, $V^{IV}O^{2+}/H_2$calm, $V^{IV}O^{2+}/H_3calc^C$, and $V^{IV}O^{2+}/H_2$calc

system	species	g_z	A_z[a]	coordination mode
$V^{IV}O^{2+}/H_3$anth	VOL	1.948	165.1	(O^-, N_{imine}, O^-); H_2O
	VOL_2H	1.951	160.7	(O^-, N_{imine}, O^-); (N_{imine}, $O^{-\,ax}$)
	VL_2H_{-2}	g_x, 1.951	A_x, 118.2	2 × (O^-, N_{imine}, O^-)
		g_y, 1.965	A_y, 48.4	
		g_z, 1.985	A_z, 17.2	
$V^{IV}O^{2+}/H_2$calm	$VOLH_{-1}$	1.950	164.9	(O^-, N_{imine}, O^-); H_2O
	VOL_2H_{-1}	1.951	160.4	(O^-, N_{imine}, O^-); (N_{imine}, $O^{-\,ax}$)
	VL_2H_{-2}	g_x, 1.950	A_x, 123.2	2 × (O^-, N_{imine}, O^-)
		g_y, 1.964	A_y, 49.2	
		g_z, 1.983	A_z, 17.6	
$V^{IV}O^{2+}/H_3calc^C$	$VOLH_{-1}$	1.948	163.7	(O^-, N_{imine}, O^-); H_2O
	VOL_2H_{-1}	1.951	160.7	(O^-, N_{imine}, O^-); (N_{imine}, $O^{-\,ax}$)
$V^{IV}O^{2+}/H_2$calc	VOL	1.947	164.9	(O^-, N_{imine}, O^-); H_2O

[a] A_x, A_y, and A_z reported in 10^{-4} cm^{-1} and in absolute value.

$V^{IV}O$ species with [(O^-, N_{arom}, O^-); H_2O] coordination.[51] Therefore, even if only one of the phenolic −OH groups (in red in Scheme 1) is deprotonated in the measurable pH range for the free ligands, the possibility to form two joined (5,6)-

dx.doi.org/10.1021/ic401080q | Inorg. Chem. 2013, 52, 8202−8213

Scheme 2. $V^{IV}O$ and V^{IV} Complexes Formed in Aqueous Solution by Anthracene Chrome Red A

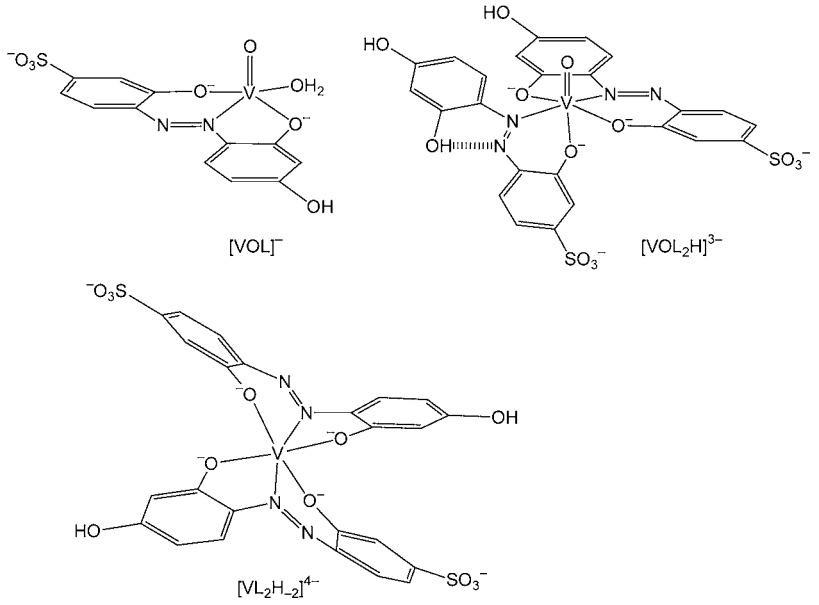

membered chelate rings induces the deprotonation of the second −OH group in the presence of the metal ion.

At pH > 5, the transformation of VOL into a species with a lower A_z value (160.4×10^{-4} cm^{-1}) is observed (**II** in Figure 3). For this complex, the potentiometry suggests the stoichiometry VOL_2H, i.e., VOL(LH); this means that the first ligand molecule is tridentate similarly to VOL with the two phenolic groups deprotonated and the "resorcinol" protonated, whereas the second one has the second phenolic group (beside the "resorcinol" one) protonated and, therefore, behaves as a bidentate ligand with the couple (N_{imine}, O^-). In this case, two coordination modes are possible: the first with the imine-N in the equatorial and the phenolate-O in the axial position, and the second one with the imine-N in the apical position in *trans* to the V=O bond. The additivity rule[50] predicts for the two different coordination modes [(O^-, N_{imine}, O^-); (N_{imine}, $O^{-\,ax}$)] and [(O^-, N_{imine}, O^-); (N_{imine}^{ax}, O^-)] 161.0 and 158.3×10^{-4} cm^{-1}, respectively. Therefore, it is more probable that the nitrogen donor occupies the equatorial plane of the $V^{IV}O^{2+}$ ion, even if the second hypothesis cannot be ruled out. The geometry of all the species formed in the system $V^{IV}O^{2+}$/H_3anth is displayed in Scheme 2. On the whole, the bis-complexes formed behave like those formed by tridentate 4-[3,5-bis(2-hydroxyphenyl)-1*H*-1,2,4-triazol-1-yl]benzoic and 4-[3,5-bis(2-hydroxyphenyl)-1*H*-1,2,4-triazol-1-yl]sulfonic acid, where the presence of two isomers has been observed.[51]

At pH > 7, the resonances of a species characterized by a very small value of A (118.2×10^{-4} cm^{-1} for anthracene chrome red A and 123.2×10^{-4} cm^{-1} for calmagite) appear. Such a value of the hyperfine coupling constant is characteristic of the non-oxido V^{IV} compounds, hexa-coordinated complexes without the double bond V=O.[1] For H_3anth, the formation of non-oxido species can be represented in this way:

$$[VOL_2H]^{3-} \leftrightarrows [VL_2H_{-2}]^{4-} + H_3O^+$$

It is important to notice that for potentiometry the non-oxido species with stoichiometry VL_2H_{-2} is indicated with VOL_2 (= $VL_2H_{-2}\cdot H_2O$, see Table 2). The non-oxido complexes $[V(anthH_{-1})_2]^{4-}$ and $[V(calmH_{-1})_2]^{2-}$ are stable in aqueous solution up to pH > 10 and are the main species at physiological pH. On the contrary, the similar ligands 4-[3,5-bis(2-hydroxyphenyl)-1*H*-1,2,4-triazol-1-yl]benzoic acid, 4-[3,5-bis(2-hydroxyphenyl)-1*H*-1,2,4-triazol-1-yl]sulfonic acid and 2,6-bis-(2-hydroxyphenyl)pyridine do not form non-oxido species at the physiological pH.[51]

The experimental EPR spectra of the non-oxido species formed by anthracene chrome red A and calmagite were simulated with the software Bruker WinEPR SimFonia[35] to extract the EPR parameters reported in Table 3. The comparison of the experimental and simulated spectrum for $[VL_2H_{-2}]^{2-}$ species of H_2calm is shown in Figure 4. The spectra are characterized by a value of A_x larger than that of the usual complexes of $V^{IV}O$ and by a smaller value of A_z. The order of the ^{51}V hyperfine coupling constants is $A_x > A_y > A_z$ and that of the g factors is $g_x < g_y < g_z < 2.0023$; such values cannot be attributed to a pure d_{xy} ground state but can be explained in terms of a mixing of d_{xy} with the excited orbitals

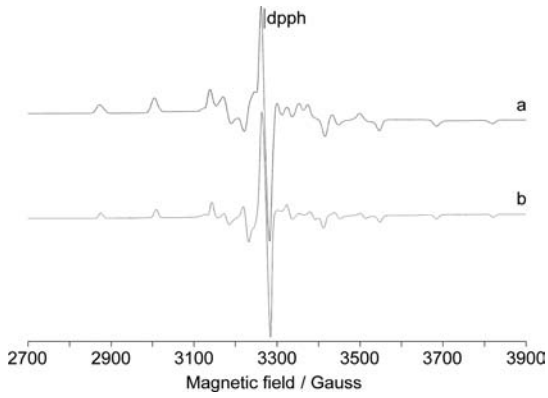

Figure 4. X-band EPR spectrum of $[V(calmH_{-1})_2]^{2-}$, recorded at pH 8.05 in the system $V^{IV}O^{2+}$/H_2calm with a total $V^{IV}O^{2+}$ concentration of 4×10^{-3} M and ligand to metal molar ratio of 10:1. (a) Experimental and (b) simulated spectrum. The parameters used for the simulation were $g_x = 1.950$, $g_y = 1.964$, $g_z = 1.983$, $A_x = -123.2 \times 10^{-4}$ cm^{-1}, $A_y = -49.2 \times 10^{-4}$ cm^{-1}, and $A_z = -17.6 \times 10^{-4}$ cm^{-1}. Diphenylpicrylhydrazyl (dpph) is used as a standard field marker ($g_{dpph} = 2.0036$).

dx.doi.org/10.1021/ic401080q | *Inorg. Chem.* 2013, 52, 8202−8213

caused by the distortion of the octahedral geometry toward the trigonal prism. However, the EPR parameters cannot be confused with those of the usual $V^{IV}O$ species ($g_z < g_x \sim g_y < 2.0023$ and $A_z \gg A_x \sim A_y$).

EPR spectra recorded on the system $V^{IV}O^{2+}/H_3calc^C$ are collected in Figure 5. H_3calc^C behaves analogously to H_3anth

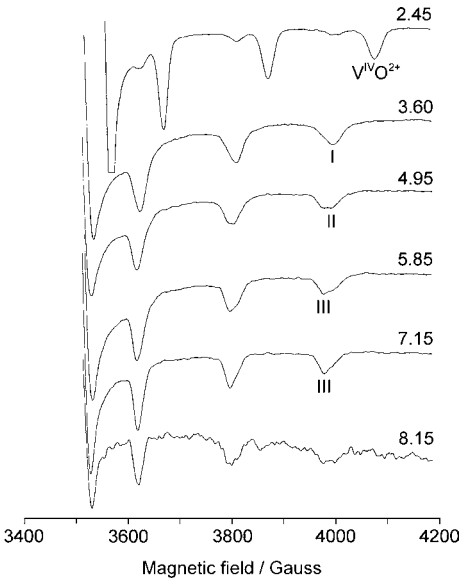

Figure 5. High field region of the X-band anisotropic EPR spectra recorded as a function of pH in the system $V^{IV}O^{2+}/H_3calc^C$ (H_3L) with a total $V^{IV}O^{2+}$ concentration of 4.0×10^{-3} M and ligand to metal molar ratio of 10:1. **I**, **II**, and **III** indicate the $M_I = 7/2$ resonances of $[VOL]^-$, $[VOLH_{-1}]^{3-}$, and $[VOL_2H_{-1}]^{5-}$, respectively.

up to the physiological pH, forming the species $[VOL]^-$ and $[VOLH_{-1}]^{2-}$ in the pH range 2.0−6.0 with the coordination mode $[(O^-, N_{imine}, O^-); H_2O]$ (**I** and **II** in Figure 5). The difference between $[VOL]^-$ and $[VOLH_{-1}]^{2-}$ is the protonation degree of the carboxylic group that undergoes deprotonation with a pK of 4.46 (Table 2). This pK value is higher than the pK_a of −COOH in the free ligand (3.96, Table 1) because in the complex there is no possibility to form a hydrogen bond between −COOH and −OH groups. At pH > 5.5, the complex $[VOL_2H_{-1}]^{5-}$ is formed (**III** in Figure 5), with one ligand tridentate with the three donors in the equatorial plane and the second ligand molecule bidentate with an equatorial−axial arrangement. The coordination mode is $[(O^-, N_{imine}, O^-); (N_{imine}, O^{-\,ax})]$ (see the discussion above-mentioned for H_3anth).

In contrast with H_3anth and H_2calm, H_3calc^C and H_2calc do not form "bare" species. Various reasons account for this different behavior: the higher charge of the bis complex of H_3calc^C ($[VOL_2H_{-1}]^{5-}$) with respect to H_3anth and H_2calm ($[VOL_2H]^{3-}$ in both the cases) disfavors significantly the deprotonation of the second phenolic group of the second coordinated ligand molecule, whereas the scarce solubility around the neutrality is the predominant factor for H_2calc.

2. Studies in the Solid State. In this study, the solid complexes $[V(dhabH_{-1})_2]$ and $[V(hmpicH_{-1})_2]$ were synthesized. The results of the elemental analysis, the dark color characteristic of the non-oxido vanadium(IV) species with phenolate-O donors, and the absence of the stretching frequency of double bond V═O, that usually falls in the range 950−1000 cm^{-1} confirm the stoichiometry proposed.

A hexa-coordinated structure formed by a tridentate ligand can be described in terms of the three isomers *meridional* (*mer*), *symmetric facial* (*sym-fac*), and *unsymmetric facial* (*unsym-fac*). The three possibilities are depicted in Scheme 3 for an (O, N, O) ligand like Hdhab and Hhmpic. For tridentate ligands with a flexible backbone a *facial* as well as a *meridional* coordination mode is possible. For example, with iminodiacetic acid the *facial* coordination is preferred,[52] whereas the reverse behavior has been reported for methylamino-*N*,*N*-bis(2-methylene-4,6-dimethylphenol).[53] On the contrary, a high rigidity of the ligand should favor the *meridional* coordination, as happens for 3,5-bis(2-hydroxyphenyl)-1-phenyl-1*H*-1,2,4-triazole (H_2hyph^{Ph}, Scheme 4) and 2,6-bis-(2-hydroxyphenyl)pyridine (H_2bhpp, Scheme 4).[51,54,55] For Hdhab and Hhmpic, an intermediate behavior is expected, and distorted geometries intermediate between the octahedron and trigonal prism can be predicted.

Scheme 3. Possible Hexa-Coordinated Vanadium(IV) Structures Formed by a Tridentate (O, N, O) Ligand: (a) *mer*, (b) *sym-fac*, and (c) *unsym-fac*

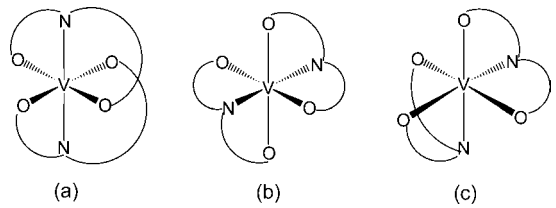

In the literature, the X-ray structures of hexa-coordinated solid metal complexes of Hdhab and Hhmpic derivatives with several metal ions, such as Cr^{III},[56] Fe^{III},[57] V^{IV},[19b,58] V^VO_2,[59] Mn^{IV},[60] Ti^{IV},[61] Co^{II},[62] Re^{IV},[63] and Sn^{IV},[64] have been reported. The structures are characterized by two chelate rings, one five- and another six-membered, with the arrangement of the ligands being usually *meridional*, but with a significant distortion toward the *facial* limit. The Ω angle formed by the two external donor atoms of the ligand with vanadium, which is 180° for *mer* and 90° for *fac* isomer, assumes values in the range 123.7−177.8° demonstrating a wide variety of geometries. Interestingly, Ω shows the minimum value for the two V^{IV} structures (123.7 and 155.8°). The structural details of the X-ray structure of $[V(dhabH_{-1})_2]$ characterized by Ludwig et al.[19b] are reported in Table 4.

An analysis performed by Favas and Kepert showed that the stereochemistry of $[ML_2]$ species formed by a tridentate ligand can be described in terms of the *normalized bite* of the ligand b^N ($b^N = 2 \times \text{sen}(\vartheta/2) = b/a$, where ϑ is the angle formed by the donor atoms with the metal ion and b and a are the bite and the mean bond length).[65] For $b^N < 1.3$, the most stable isomer is the *mer* one. For $b^N > 1.5$, the minimum energy corresponds to the *unsym-fac* form, whereas for intermediate situations with $1.3 < b^N < 1.5$, the energy of the three isomers is comparable and all three structures are possible.

The geometry of $[V(dhab_{-1})_2]$ and $[V(hmpic_{-1})_2]$ was optimized with the Gaussian 09 software through DFT methods, using the functional B3P86 and the valence triple-ζ basis set 6-311g, according to the procedure reported in the literature.[40]

DFT simulations allow us to evaluate the relative stability of the three isomers in MeOH (the solvent where they were isolated), through the calculation of the difference between the Gibbs free energy in solution (ΔG^{tot}_{sol}).[43e,46b,66] The data

dx.doi.org/10.1021/ic401080q | Inorg. Chem. 2013, 52, 8202−8213

Scheme 4. Ligands That Form the Non-Oxido V^{IV} Species, Whose EPR Behavior Was Compared in This Study with That of H_3anth, H_2calm, Hdhab, and Hhmpic (Donor Atoms Are Represented in Red)

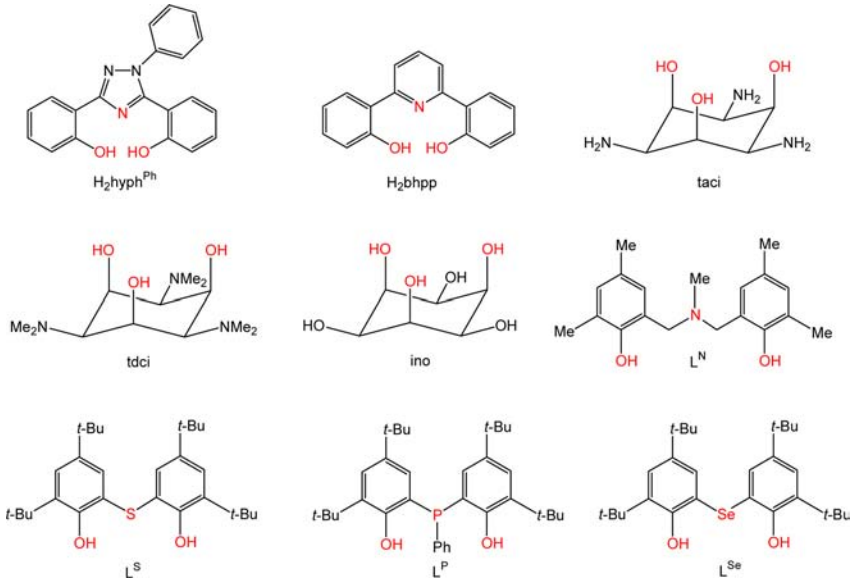

Table 4. ΔG Values at 298.15 K in the Gas Phase and MeOH for the Three Isomers of $[V(dhab_{-1})_2]$ and $[V(hmpic_{-1})_2]$[a,b]

reaction	ΔG^{tot}_{gas}	$\Delta(\Delta G^{solv})^c$	$\Delta(\Delta G^{solv})^d$	$\Delta G^{tot}_{sol}{}^c$	$\Delta G^{tot}_{sol}{}^d$
mer → *unsym-fac* (Hdhab)	−1.9	−12.8	−2.9	−14.7	−4.8
sym-fac → *unsym-fac* (Hdhab)	−262.6	−1.0	4.9	−263.6	−257.7
mer → *unsym-fac* (Hmpic)	11.0	−14.9	−11.9	−3.9	−1.0
sym-fac → *unsym-fac* (Hmpic)	−201.7	−3.2	−7.5	−209.2	−204.9

[a]Energies reported in kJ mol^{-1}. [b]Calculations performed at the level of theory B3P86/6-311g. [c]SMD model with MeOH as solvent. [d]PCM with MeOH as solvent.

obtained indicate that for $[V(dhab_{-1})_2]$ and $[V(hmpic_{-1})_2]$ the stability order of the three possible isomers in aqueous solution is *unsym-fac* > *mer* ≫ *sym-fac*. The free energy difference between the *unsym-fac* and *mer* arrangements of $[V(dhab_{-1})_2]$ and $[V(hmpic_{-1})_2]$ is 14.7 and 3.9 kJ/mol (SMD) and 4.8 and 1.0 kJ/mol (PCM). In the gas phase, the order is *unsym-fac* > *mer* ≫ *sym-fac* for $[V(dhab_{-1})_2]$ and *mer* > *unsym-fac* ≫ *sym-fac* for $[V(hmpic_{-1})_2]$. For $[V(hmpic_{-1})_2]$, the free energy of solvation favors the *unsym-fac* and renders this isomer more stable than the *mer* in MeOH. Overall, the data obtained in the framework of the SMD and PCM model give the same qualitative description. The small value of ΔG^{tot}_{sol} for the transformation of *mer* to *unsym-fac* species confirms that the two isomers have comparable energy: therefore, in the solid state several factors, such as the intermolecular hydrogen bonds and packing effects, contribute to determine the most stable structure. The slightly higher stability of *unsymmetric facial* than *meridional* coordination for V^{IV} complexes, suggested by the DFT data, is confirmed by X-ray diffractometric analysis of $[V(onmsb)_2]$, where H_2onmsb is *N*-(2-oxido-1-naphthylmethylene)-2′-sulfidobenzimine, a tridentate (O, N, S) ligand structurally similar to Hdhab.[67]

The structures of $[V(dhabH_{-1})_2]$ and $[V(hmpicH_{-1})_2]$ are shown in Figure 6. In Table 5, the main structural details and

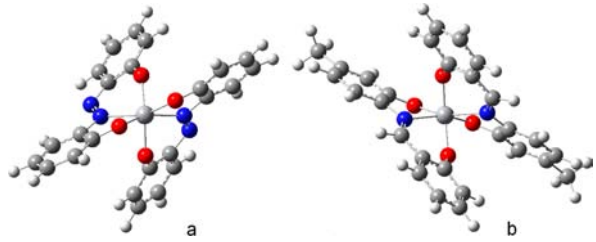

Figure 6. Structures of (a) $[V(dhab_{-1})_2]$ and (b) $[V(hmpic_{-1})_2]$ optimized with DFT methods at the B3P86/6-311g level of theory.

geometrical parameters calculated for $[V(dhabH_{-1})_2]$, $[V(hmpicH_{-1})_2]$, $[V(anthH_{-1})_2]^{4-}$, and $[V(calmH_{-1})_2]^{2-}$ are reported. An important structural parameter to characterize the geometry of hexa-coordinated V^{IV} species is the twist angle Φ, in our case defined as the angle between the two triangular faces of the coordination polyhedron (0.0° for a trigonal prism with the two triangles eclipsed and 60.0° for a regular octahedron with the two triangles staggered).

It can be noticed that the *unsymmetric facial* geometry results in a significant distortion of the structure toward the trigonal prism with respect to the complexes with VO_4N_2 coordination with *meridional* arrangement formed by 3,5-bis-(2-hydroxyphenyl)-1-phenyl-1*H*-1,2,4-triazole and 2,6-bis-(2-hydroxyphenyl)pyridine (Φ of 55.0 and 59.6°, respectively[51]).

The data calculated in Table 5 for the structures of $[V(dhab_{-1})_2]$ and $[V(hmpic_{-1})_2]$ were compared with those of $[V(dhab_{-1})_2]$, whose X-ray diffraction analysis has been reported in the literature.[19b] From an examination of Table 5, it can be noticed that the *unsymmetric facial* coordination can be associated with an octahedral geometry distorted toward the trigonal prism with values of the angles Φ and Θ much smaller than 60 and 180°, respectively. The angle Ω formed by the external donors with vanadium is indicative of the arrangement of the ligand with respect to the metal ion; of course, it is 180° for *mer* and 90° for *fac* isomers and assumes the values of 119.2,

dx.doi.org/10.1021/ic401080q | Inorg. Chem. 2013, 52, 8202−8213

Table 5. Geometrical Parameters Obtained by DFT Methods for Non-Oxido V^{IV} Compounds and Comparison with X-Ray Structure of $[V(dhabH_{-1})_2]$[a]

	calculated				experimental
complex	$[V(anthH_{-1})_2]^{4-}$[b]	$[V(calmH_{-1})_2]^{2-}$[b]	$[V(dhabH_{-1})_2]$[b]	$[V(hmpicH_{-1})_2]$[b]	$[V(dhabH_{-1})_2]$[c]
isomer	*unsym-fac*	*unsym-fac*	*unsym-fac*	*unsym-fac*	*unsym-fac*
b^N[d]	1.278	1.250	1.275	1.267	1.287
V−O	1.877, 1.899; 1.877, 1.899	1.865, 1.889; 1.865, 1.889	1.877, 1.885; 1.877, 1.885	1.875, 1.882; 1.875, 1.882	1.883, 1.894; 1.891, 1.900
V−N	2.164, 2.164	2.171, 2.171	2.155, 2.155	2.166, 2.166	2.109, 2.116
O−V−O	119.6, 119.6	116.0, 116.0	119.2, 119.2	117.4, 117.4	123.3, 124.2
N−V−N	116.6	114.4	118.1	117.3	120.3
Φ[e]	36.2	41.4	35.9	37.5	28.8
Θ[f]	151.9	155.3	151.6	153.6	146.2
Ω[g]	119.6	116.0	119.2	117.4	123.7
ψ[h]	79.5	77.3	79.2	77.2	81.7

[a]Distance in Å and angles in deg. [b]Structure simulated through DFT methods at the level of theory B3P86/6-311g. [c]Experimental structure reported in ref 19b. [d]*Normalized bite*. [e]Twist angle: 60° for octahedral and 0° for trigonal prismatic geometry. [f]Angle formed by the donors in *trans* position with vanadium (mean value): 180° for octahedral and 135° for trigonal prismatic geometry. [g]Angle formed by the two external donor atoms of the ligand with vanadium (mean value): 180° for *mer* and 90° for *fac* isomers. [h]Angle formed by the two external donors of the ligand with the central one (mean value).

117.4, 119.6, and 116.0° for $[V(dhabH_{-1})_2]$, $[V(hmpicH_{-1})_2]$, $[V(anthH_{-1})_2]^{4-}$, and $[V(calmH_{-1})_2]^{2-}$, respectively. Finally, for $b^N < 1.414$, the angle ψ formed by two external donors of the ligand (O atoms) with the central one (N atom) follows the order *mer* ≫ *unsym-fac* > *sym-fac* (see ref 65) and the values for $[V(dhab_{-1})_2]$ and $[V(hmpic_{-1})_2]$ are smaller than those of *meridional* structures of 3,5-bis-(2-hydroxyphenyl)-1-phenyl-1*H*-1,2,4-triazole and 2,6-bis-(2-hydroxyphenyl)pyridine (88.0 and 85.1°, respectively[51]).

3. Prediction of the ^{51}V Hyperfine Coupling Constants and Electronic Structure of V^{IV} Species and Their Relationship with the Geometric Parameters. The solid non-oxido vanadium(IV) complexes can be characterized by EPR spectroscopy. The experimental spectra of $[V(dhab_{-1})_2]$ and $[V(hmpic_{-1})_2]$ are comparable to those of the species formed in aqueous solution by the structurally similar ligands H_3anth and H_2calm, $[V(anthH_{-1})_2]^{4-}$ and $[V(calmH_{-1})_2]^{2-}$. It must be noticed that the spectra resemble closely those of a $V^{IV}O$ species (characterized by d_{xy} ground state), except for the significantly low value of $|A_i|$ (i = *x*, *z*). The spectrum of $[V(dhab_{-1})_2]$ and the comparison with the simulated one is shown in Figure 7. EPR spectra of hexa-coordinated vanadium-(IV) complexes can be divided into two groups: those with $g_z \ll g_x \sim g_y < 2.0023$ and $A_z \gg A_x \sim A_y$ (d_{xy} ground state) and those with $g_x \sim g_y \ll g_z \sim 2.0023$ and $A_z \ll A_x \sim A_y$ (d_{z^2} ground state).[25] On the basis of spectroscopic data, $[V(anthH_{-1})_2]^{4-}$, $[V(calmH_{-1})_2]^{2-}$, $[V(dhab_{-1})_2]$, and $[V(hmpic_{-1})_2]$ fall in the first group, and a singly occupied molecular orbital (SOMO) based on V-d_{xy} is predicted.

Nowadays, the prediction of ^{51}V hyperfine coupling constant tensor $\boldsymbol{A}$ is possible through the DFT methods. We recently noticed that the ORCA software gives better results than the popular Gaussian for non-oxido vanadium(IV) complexes, because it includes the second-order spin−orbit effects (see DFT calculations in the Experimental and Computational Section), whose contribution to A values is more important than for $V^{IV}O$ species (see below).[51] In this work, we used the PBE0 functional and VTZ basis set. The results are listed in Table 6.

It can be noted that for $[V(anthH_{-1})_2]^{4-}$, $[V(calmH_{-1})_2]^{2-}$, and $[V(dhab_{-1})_2]$, the order $A_x \gg A_y \gg A_z$ is predicted, whereas for $[V(hmpic_{-1})_2]$, $A_z \gg A_y \gg A_x$. Such an order in

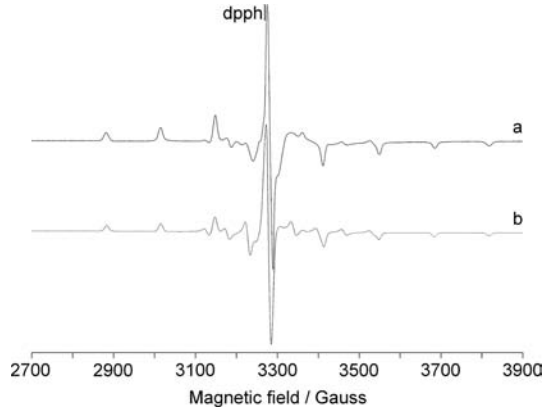

Figure 7. X-band anisotropic EPR spectrum of $[V(dhabH_{-1})_2]$: (a) experimental and (b) simulated. The parameters used for the simulation were $g_x = 1.951$, $g_y = 1.962$, $g_z = 1.982$, $A_x = -122.4 \times 10^{-4}$ cm^{-1}, $A_y = -52.8 \times 10^{-4}$ cm^{-1}, and $A_z = -18.0 \times 10^{-4}$ cm^{-1}. Diphenylpicrylhydrazyl (dpph) is used as a standard field marker ($g_{dpph} = 2.0036$).

the value of A_i results in a spectrum that resembles that of a $V^{IV}O$ species, in agreement with what is observed (see Figures 4 and 7). The prediction of A_x for $[V(anthH_{-1})_2]^{4-}$, $[V(calmH_{-1})_2]^{2-}$, and $[V(dhab_{-1})_2]$ and A_z for $[V(hmpic_{-1})_2]$ (mean deviation from the experimental value of −6.8%) appears to be less good than that for $V^{IV}O$ complexes, for which deviations below 3% are obtained.[43a,f] This can be ascribed to the second-order spin−orbit contribution to A for "bare" V^{IV} species that represents 6−7% of A_x or A_z. The deviations found are comparable with those of the non-oxido V^{IV} species formed by H_2hyph^{Ph} and H_2bhpp (Scheme 4) recently described.[51] The possibility to calculate the values of A_x^{SO} and A_z^{SO} with ORCA accounts for its better performance than Gaussian.

As is known, the ^{51}V hyperfine coupling constant along the *z* axis (A_z) for a $V^{IV}O$ species can be predicted through the application of the empiric "additivity rule" from the sum of the contributions of each equatorial donor with deviations generally smaller than $\sim 3 \times 10^{-4}$ cm^{-1} with respect to the experimental value.[50] On the contrary, the prediction of the hyperfine coupling constants of a non-oxido V^{IV} species is not possible *a priori*. In the literature, the A values were put in a relationship

dx.doi.org/10.1021/ic401080q | Inorg. Chem. 2013, 52, 8202−8213

Table 6. ^{51}V Hyperfine Coupling Constants Calculated through DFT Methods (with ORCA Software) for Non-Oxido Vanadium(IV) Complexes[a]

complex	A^{FC}	A_x^D	A_y^D	A_z^D	A_x^{SO}	A_y^{SO}	A_z^{SO}	A_{iso}	A_x	A_y	A_z	A_i^{exptl}[b]	dev. %[c]
$[V(anthH_{-1})_2]^{4-}$	−57.5	−47.1	−8.2	55.3	−7.3	−9.0	−2.1	−63.6	−111.9	−74.7	−4.3	−118.2	−5.3
$[V(calmH_{-1})_2]^{2-}$	−54.0	−49.2	−4.2	53.3	−7.5	−8.5	−2.2	−60.1	−110.7	−66.7	−2.9	−123.2	−10.1
$[V(dhab_{-1})_2]$	−55.6	−51.6	−1.8	53.4	−7.4	−8.1	−2.1	−61.5	−114.6	−65.5	−4.4	−122.4	−6.4
$[V(hmpic_{-1})_2]$	−54.7	51.7	3.1	−54.8	−2.4	−7.8	−7.9	−60.7	−5.4	−59.4	−117.4	−124.2	−5.5

[a]Values reported in 10^{-4} cm^{-1}. [b]i = x for $[V(anthH_{-1})_2]^{4-}$, $[V(calmH_{-1})_2]^{2-}$, and $[V(dhab_{-1})_2]$ and z for $[V(hmpic_{-1})_2]$. [c]Percent deviation from the experimental value calculated as $100 \times (|A_i|^{calcd} - |A_i|^{exptl})/|A_i|^{exptl}$, with i = x or z.

with the trigonal prismatic distortion of the hexa-coordinated structure.[25] With bidentate (O, O) ligands, structures distorted toward the trigonal prism are obtained and the order $A_z \ll A_x \sim A_y$ is found, with A_x and A_y in the range $(100-120) \times 10^{-4}$ cm^{-1} and A_z much smaller than 20×10^{-4} cm^{-1}.[68,69] Amavadin is an octahedral complex and shows another type of spectroscopic behavior with $A_z \gg A_x \sim A_y$.[70] To verify if a correlation between the value of Φ and A is possible, in this work we analyzed 13 non-oxido V^{IV} structures formed by tridentate (O, O, O), (O, N, O), (O, S, O), (O, P, O), and (O, Se, O) ligands: H_3anth, H_2calm, Hdhab, and Hhmpic studied in this paper; H_2hyph^{Ph} and H_2bhpp;[51] taci (1,3,5-triamino-1,3,5-trideoxy-*cis*-inositol) and tdci (1,3,5-trideoxy-1,3,5-tris-(dimethylamino)-*cis*-inositol);[21a] ino (*cis*-inositol);[21b] and bis-phenol L^N, L^S, L^P, and L^{Se} derivatives studied by the Chaudhuri group (Scheme 4).[19c,20]

The arrangement of the ligands can be *meridional* (H_2hyph^{Ph}, H_2bhpp, and L^N) or *facial* (H_3anth, H_2calm, Hdhab, Hhmpic, taci, tdci, ino, L^S, L^P, and L^{Se}) and the geometry octahedral (H_2hyph^{Ph}, H_2bhpp, taci, tdci, ino, L^N, L^S, L^P, and L^{Se}) or distorted toward the trigonal prism (H_3anth, H_2calm, Hdhab, and Hhmpic). In Figure S1 of the Supporting Information, the largest value of A is depicted as a function of Φ. It can be easily noticed that no correlation exists; actually, the points seem to be in random order. Rather surprisingly, the values of A_i for the species with a Φ close to the octahedral geometry are different and can be very large, as those of $[V(L^N)_2]$ and $[V(hyph^{Ph})_2]$ (147.0 and 142.0×10^{-4} cm^{-1}), and very small, as those of the species formed by cyclic derivatives of *cis*-inositol, $[V(taci)_2]^{4+}$, $[V(tdci)_2]^{4+}$, and $[V(inoH_{-3})_2]^{2-}$ (99.4, 96.1, and 99.1×10^{-4} cm^{-1}, respectively). This means that the distortion of a hexa-coordinated V^{IV} species is not the most important factor which determines its electronic structure and, hence, its EPR spectrum.

Recently, we noticed that the arrangement of the ligand molecules, *mer* or *fac*, has marked effects on the electronic structure of a non-oxido V^{IV} complex.[51] In particular, the values of A can be correlated with the angle Ω, i.e., the angle formed by the two external donors of the tridentate ligand with V, which is 180° for a *mer* isomer and 90° for a *fac* isomer (see above). The values of A_i as a function of Ω are shown in Figure 8.

From an examination of Figure 8, it emerges that a correlation between A_i and Ω exists. The 13 complexes can be divided into three groups: the *meridional* structures (H_2hyph^{Ph}, H_2bhpp, and L^N), the *facial* structures formed by open-chain ligands (H_3anth, H_2calm, Hdhab, Hhmpic, L^S, L^P, and L^{Se}), and the *facial* structures formed by cyclic ligands (taci, tdci, and ino). The reason for which the *facial* complexes fall into two different groups is that the cyclic ligands such as taci, tdci, and ino impose a less flexible geometry to the metal ion. It is clear that the geometric arrangement of the ligands (*mer* or *fac*) influences significantly the ^{51}V hyperfine coupling tensor $\mathbf{A}$. On the basis of these data, this factor seems to be more effective than the twist angle Φ on the electronic structure of the complexes.

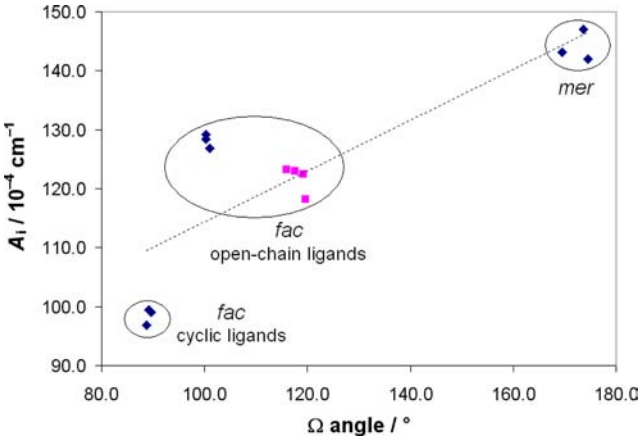

Figure 8. A_i values for non-oxido V^{IV} complexes as a function of the angle Ω. The pink squares indicate $[V(anthH_{-1})_2]^{4-}$, $[V(calmH_{-1})_2]^{2-}$, $[V(dhab_{-1})_2]$, and $[V(hmpic_{-1})_2]$. A_i (i = x or z) represents the largest values of the ^{51}V hyperfine coupling tensor $\mathbf{A}$. The dotted gray line represents the best linear fitting of the 13 points.

The subsequent step was the analysis of the spin density on V d orbitals (Table 7). The spin density was calculated choosing a coordinate system in which the z axis is roughly oriented along the two V−O bonds and the x and y axes along the O−V−N directions (see DFT calculation in the Experimental and Computational Section). For a $V^{IV}O$ complex with distorted octahedral or square pyramidal geometry, the energy order of the five d orbitals is $d_{xy} < d_{xz} \sim d_{yz} < d_{x^2-y^2} < d_{z^2}$,[71,72] the SOMO being the d_{xy} orbital. For a non-oxido V^{IV} species with a hexa-coordinated geometry distorted toward the trigonal prism, an increasing mixing of d_{xy} with the excited orbitals, mainly with d_{z^2}, is expected.[25] As a consequence, the spin density on d_{xy} and the value of A should decrease.

The data reported in Table 7 demonstrate that most of the spin density is in the d_{xy} orbital, with a significant part in the d_{z^2} orbital. This suggests the mixing between d_{xy} and d_{z^2} orbitals, in agreement with what is expected.[25] In Figure 9, the values of A_i for the non-oxido V^{IV} complexes as a function of the spin density on the V d_{xy} orbital are represented. A linear correlation is obtained with an R^2 value of 0.96. In this case too, the 13 V^{IV} species analyzed can be grouped into *meridional* and *facial* isomers; in their turn, the *facial* isomers can be further divided into those formed by open-chain and those formed by cyclic ligands. It is noteworthy that the three cyclic ligands (taci, tdci, and ino) form almost perfect octahedral geometries,[21] but this does not result in a pure d_{xy} ground state due to significant mixing with the d_{z^2} orbital. In other words, the electronic

dx.doi.org/10.1021/ic401080q | Inorg. Chem. 2013, 52, 8202−8213

Table 7. Spin Density on V d Orbitals for $[V(anthH_{-1})_2]^{4-}$, $[V(calmH_{-1})_2]^{2-}$, $[V(dhab_{-1})_2]$, and $[V(hmpic_{-1})_2]$

complex	d_{z^2}	d_{xz}	d_{yz}	$d_{x^2-y^2}$	d_{xy}	total d
$[V(anthH_{-1})_2]^{4-}$	0.165	0.097	0.078	0.083	0.747	1.170
$[V(calmH_{-1})_2]^{2-}$	0.146	0.099	0.082	0.069	0.779	1.175
$[V(dhab_{-1})_2]$	0.156	0.099	0.082	0.085	0.736	1.158
$[V(hmpic_{-1})_2]$	0.140	0.108	0.089	0.080	0.739	1.156

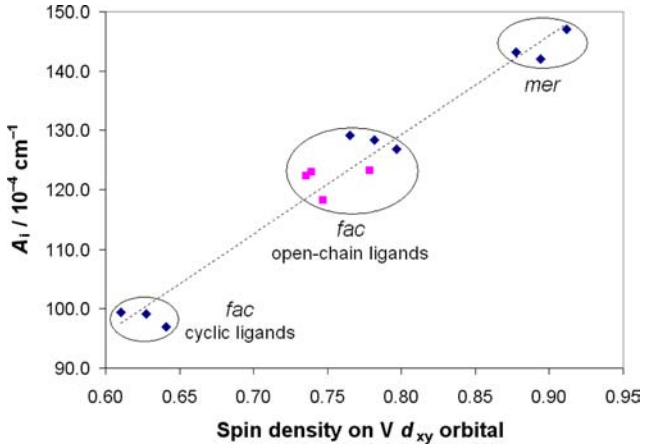

Figure 9. A_i values for non-oxido V^{IV} complexes as a function of the spin density on the V d_{xy} orbital. The pink squares indicate $[V(anthH_{-1})_2]^{4-}$, $[V(calmH_{-1})_2]^{2-}$, $[V(dhab_{-1})_2]$, and $[V(hmpic_{-1})_2]$. A_i ($i = x$ or z) is the largest values of the ^{51}V hyperfine coupling tensor **A**. The dotted gray line represents the best linear fitting of the 13 points.

configuration of the non-oxido V^{IV} species is strongly influenced from the structural features of the ligands (on which the type of arrangement, *mer* or *fac*, depends) that, in their turn, determine the geometry of the complexes.

The lowering of the A_i value due to a decrease of the spin density on the V d_{xy} orbital is not unexpected. In fact, the decrease of A_i (for simplicity, we will consider the situation with $i = z$) in the case of a linear combination of d_{xy} and d_{z^2} orbitals can be explained considering the expressions for A_z when SOMO is a pure d_{xy} or d_{z^2} orbital (eqs 1 and 2):[73]

$$d_{xy}: A_z = P_d\left[\beta^2\left(-\kappa - \frac{4}{7}\right) + (g_z - 2.0023) + \frac{3}{14}(g_x - 2.0023) + \frac{3}{14}(g_y - 2.0023)\right] \quad (1)$$

$$d_{z^2}: A_z = P_d\left[\delta^2\left(-\kappa + \frac{4}{7}\right) - \frac{1}{14}(g_x - 2.0023) - \frac{1}{14}(g_y - 2.0023)\right] \quad (2)$$

P_d is the dipolar term—$g_e g_N \beta_e \beta_N \langle r\rangle^{-3}$, with $\langle r\rangle$ the mean distance of the electron from the nucleus—and is 128×10^{-4} cm^{-1} for the V^{IV} ion,[74] and κ is the isotropic or Fermi contact and is 0.85.[74] β and δ are the coefficients of the atomic orbital in the SOMO.

It must be noticed that when the SOMO is the d_{xy} orbital, the four terms inside the square parentheses are negative (g_x, g_y, and g_z are always smaller than 2.0023): therefore, the value of A_z will be negative and large in absolute value. On the contrary, when the SOMO is d_{z^2}, the first term ($\delta^2(-\kappa + 4/7)$) is negative but small in absolute value, whereas the second and third terms ($-1/14(g_x - 2.0023) - 1/14(g_y - 2.0023)$) inside the square parentheses are positive and smaller in absolute value than the corresponding terms in eq 1 for the d_{xy} case. As a consequence, the value of A_z when the SOMO is d_{z^2} (eq 2) will be smaller in absolute value than that expected when the SOMO is the d_{xy} orbital (eq 1). Therefore, the mixing of the V d_{xy} orbital with d_{z^2} in the SOMO will cause a lowering of the absolute value (experimentally measured) of the ^{51}V hyperfine coupling constant along the z axis.

CONCLUSIONS

The number of non-oxido V^{IV} complexes is very small with respect to $V^{IV}O$ species, especially in aqueous solution. The synthesis of these complexes requires a strong ligand, usually provided by phenolate- or alcoholate-O^- or thiolate-S^-, able to compensate for the breaking of the V=O bond. In this work, the formation of "bare" V^{IV}, formed by tridentate (O^-, N_{imine}, O^-) ligands, is unambiguously proved in aqueous solution around the physiological pH and in the solid state. The flexibility of the ligands results in an *unsymmetric facial* coordination with a geometry intermediate between the octahedron and the trigonal prism.

EPR spectroscopy is an important tool that can be used to distinguish a V^{IV} from a $V^{IV}O$ species. In particular, the largest ^{51}V hyperfine coupling constant of a V^{IV} complex (usually <140 $\times 10^{-4}$ cm^{-1}) is much smaller than that of a $V^{IV}O$ compound (usually >150 $\times 10^{-4}$ cm^{-1}). DFT calculations can predict the A_i values and distinguish the two situations. A value of A_i much smaller than 140×10^{-4} cm^{-1} has been correlated in the literature with the distortion of the hexa-coordinated structure from an octahedron toward to the trigonal prism. In this work, we highlight that for tridentate ligands A_i cannot be put in a relationship with the parameter connected to this distortion (the twist angle Φ) but only with the arrangement of the two molecules around V, *meridional* or *facial*; in particular, V^{IV} complexes formed by cyclic ligands that stabilize octahedral geometry (those derived from *cis*-inositol,[21] see Figure S1 of the Supporting Information) are those with the smallest values of A_i. The specific arrangement of the ligands (*mer* or *fac*) influences the electronic structure of the complex and causes a more or less significant mixing between the V d_{xy} and d_{z^2} orbitals, such a mixing being the greatest for the *facial* isomers. The mixing of d_{z^2} with a d_{xy} orbital results in a lowering of the A_i value; in particular, the higher the mixing, the greater the lowering of A_i. A parameter that can be satisfactorily correlated with the A_i values is the spin density on the V d_{xy} orbital, which can be easily calculated with DFT simulations. Therefore, the EPR behavior of rare non-oxido V^{IV} species can be rationalized in terms of the isomerism of the hexa-coordinated species and spin density on V d orbitals.

dx.doi.org/10.1021/ic401080q | Inorg. Chem. 2013, 52, 8202−8213

■ ASSOCIATED CONTENT

Supporting Information

A_i values for non-oxido V^{IV} complexes as a function of the twist angle Φ. This material is available free of charge via the Internet at http://pubs.acs.org.

■ AUTHOR INFORMATION

Corresponding Author

*E-mail: garribba@uniss.it (E.G.).

Notes

The authors declare no competing financial interest.

■ ACKNOWLEDGMENTS

This research was supported by the Hungarian Scientific Research Fund (K 72956) and TÁMOP (4.2.4.A/2-11-1-2012-0001) and it was realized in the frames of TÁMOP 4.2.4. A/2-11-1-2012-0001 "National Excellence Program-Elaborating and operating an inland student and researcher personal support system".

■ REFERENCES

(1) Rehder, D. *Bioinorganic Vanadium Chemistry*. John Wiley & Sons, Ltd: Chichester, U. K., 2008.

(2) (a) Vilter, H. In *Met. Ions Biol. Syst.*; Sigel, H., Sigel, A., Eds.; Marcel Dekker: New York, 1995; Vol. *31*, pp 325−362. (b) Pecoraro, V. L.; Slebodnick, C.; Hamstra, B. In *Vanadium Compounds*; American Chemical Society: Washington, DC, 1998; Vol. *711*, pp 157−167.

(3) (a) Robson, R. L.; Eady, R. R.; Richardson, T. H.; Miller, R. W.; Hawkins, M.; Postgate, J. R. *Nature* **1986**, *322*, 388−390. (b) Eady, R. R. *Coord. Chem. Rev.* **2003**, *237*, 23−30.

(4) (a) Ueki, T.; Michibata, H. *Coord. Chem. Rev.* **2011**, *255*, 2249−2257. (b) Fattorini, D.; Regoli, F. In *Vanadium. Biochemical and Molecular Biological Approaches*; Michibata, H., Ed.; Springer: Netherlands, 2012; pp 73−92.

(5) Crans, D. C.; Smee, J. J.; Gaidamauskas, E.; Yang, L. *Chem. Rev.* **2004**, *104*, 849−902.

(6) Costa Pessoa, J.; Tomaz, I. *Curr. Med. Chem.* **2010**, *17*, 3701−3738.

(7) Rehder, D. *Future Med. Chem.* **2012**, *4*, 1823−1837.

(8) (a) Sanna, D.; Micera, G.; Garribba, E. *Inorg. Chem.* **2009**, *48*, 5747−5757. (b) Sanna, D.; Micera, G.; Garribba, E. *Inorg. Chem.* **2010**, *49*, 174−187. (c) Sanna, D.; Buglyó, P.; Micera, G.; Garribba, E. *J. Biol. Inorg. Chem.* **2010**, *15*, 825−839. (d) Sanna, D.; Micera, G.; Garribba, E. *Inorg. Chem.* **2011**, *50*, 3717−3728. (e) Sanna, D.; Biro, L.; Buglyo, P.; Micera, G.; Garribba, E. *Metallomics* **2012**, *4*, 33−36. (f) Sanna, D.; Bíró, L.; Buglyó, P.; Micera, G.; Garribba, E. *J. Inorg. Biochem.* **2012**, *115*, 87−99.

(9) (a) Willsky, G. R.; Goldfine, A. B.; Kostyniak, P. J.; McNeill, J. H.; Yang, L. Q.; Khan, H. R.; Crans, D. C. *J. Inorg. Biochem.* **2001**, *85*, 33−42. (b) Liboiron, B. D.; Thompson, K. H.; Hanson, G. R.; Lam, E.; Aebischer, N.; Orvig, C. *J. Am. Chem. Soc.* **2005**, *127*, 5104−5115. (c) Kiss, T.; Jakusch, T.; Hollender, D.; Dörnyei, A. In *Vanadium: The Versatile Metal*; American Chemical Society: Washington, DC, 2007; Vol. *974*, pp 323−339. (d) Kiss, T.; Jakusch, T.; Hollender, D.; Dornyei, A.; Enyedy, E. A.; Pessoa, J. C.; Sakurai, H.; Sanz-Medel, A. *Coord. Chem. Rev.* **2008**, *252*, 1153−1162. (e) Jakusch, T.; Hollender, D.; Enyedy, E. A.; Gonzalez, C. S.; Montes-Bayon, M.; Sanz-Medel, A.; Pessoa, J. C.; Tomaz, I.; Kiss, T. *Dalton Trans.* **2009**, 2428−2437. (f) Jakusch, T.; Pessoa, J. C.; Kiss, T. *Coord. Chem. Rev.* **2011**, *255*, 2218−2226. (g) Correia, I.; Jakusch, T.; Cobbinna, E.; Mehtab, S.; Tomaz, I.; Nagy, N. V.; Rockenbauer, A.; Costa Pessoa, J.; Kiss, T. *Dalton Trans.* **2012**, *41*, 6477−6487. (h) Mehtab, S.; Gonçalves, G.; Roy, S.; Tomaz, A. I.; Santos-Silva, T.; Santos, M. F. A.; Romão, M. J.; Jakusch, T.; Kiss, T.; Costa Pessoa, J. *J. Inorg. Biochem.* **2013**, *121*, 187−195. (i) Gonçalves, G.; Tomaz, A. I.; Correia, I.; Veiros, L. F.; Castro, M. M. C. A.; Avecilla, F.; Palacio, L.; Maestro, M.; Kiss, T.; Jakusch, T.; Garcia, M. H. V.; Costa Pessoa, J. *Dalton Trans.* DOI: 10.1039/c3dt50553g.

(10) (a) Nielsen, F. H. In *Vanadium Compounds: Chemistry, Biochemistry and Therapeutic Applications*; American Chemical Society: Washington, DC, 1998; Vol. *711*, pp 297−307. (b) Kustin, K.; Robinson, W. E. In *Met. Ions Biol. Syst.*; Sigel, H., Sigel, A., Eds.; Marcel Dekker: New York, 1995; Vol. *31*, pp 511−542.

(11) (a) Kustin, K.; Toppen, D. L. *Inorg. Chem.* **1973**, *12*, 1404−1407. (b) Cantley, L. C.; Ferguson, J. H.; Kustin, K. *J. Am. Chem. Soc.* **1978**, *100*, 5210−5212. (c) Sakurai, H.; Shimomura, S.; Ishizu, K. *Inorg. Chim. Acta* **1981**, *55*, L67−L69. (d) Sreedhara, A.; Susa, N.; Rao, C. P. *Inorg. Chim. Acta* **1997**, *263*, 189−194. (e) Baran, E. J. *J. Inorg. Biochem.* **2000**, *80*, 1−10. (f) Wilkins, P. C.; Johnson, M. D.; Holder, A. A.; Crans, D. C. *Inorg. Chem.* **2006**, *45*, 1471−1479.

(12) Allen, F. H.; Kennard, O. *Chem. Des. Autom. News* **1993**, *8*, 31−37.

(13) (a) Bayer, E.; Kneifel, H. *Z. Naturforsch., B: Anorg. Chem., Org. Chem., Biochem., Biophys., Biol.* **1972**, *27*, 207−207. (b) Bayer, E.; Koch, E.; Anderegg, G. *Angew. Chem., Int. Ed. Engl.* **1987**, *26*, 545−546.

(14) Berry, R. E.; Armstrong, E. M.; Beddoes, R. L.; Collison, D.; Ertok, S. N.; Helliwell, M.; Garner, C. D. *Angew. Chem., Int. Ed.* **1999**, *38*, 795−797.

(15) Sutradhar, M.; Mukherjee, G.; Drew, M. G. B.; Ghosh, S. *Inorg. Chem.* **2007**, *46*, 5069−5075.

(16) Klich, P. R.; Daniher, A. T.; Challen, P. R.; McConville, D. B.; Youngs, W. J. *Inorg. Chem.* **1996**, *35*, 347−356.

(17) (a) Cooper, S. R.; Koh, Y. B.; Raymond, K. N. *J. Am. Chem. Soc.* **1982**, *104*, 5092−5102. (b) Karpishin, T. B.; Stack, T. D. P.; Raymond, K. N. *J. Am. Chem. Soc.* **1993**, *115*, 182−192.

(18) (a) Stiefel, E. I.; Dori, Z.; Gray, H. B. *J. Am. Chem. Soc.* **1967**, *89*, 3353−3354. (b) Broderick, W. E.; McGhee, E. M.; Godfrey, M. R.; Hoffman, B. M.; Ibers, J. A. *Inorg. Chem.* **1989**, *28*, 2902−2904. (c) Kondo, M.; Minakoshi, S.; Iwata, K.; Shimizu, T.; Matsuzaka, H.; Kamigata, N.; Kitagawa, S. *Chem. Lett.* **1996**, *25*, 489−490.

(19) (a) Diamantis, A. A.; Snow, M. R.; Vanzo, J. A. *J. Chem. Soc., Chem. Commun.* **1976**, 264−265. (b) Ludwig, E.; Hefele, H.; Uhlemann, E.; Weller, F.; Kläi, W. *Z. Anorg. Allg. Chem.* **1995**, *621*, 23−28. (c) Paine, T. K.; Weyhermüller, T.; Bill, E.; Bothe, E.; Chaudhuri, P. *Eur. J. Inorg. Chem.* **2003**, 4299−4307.

(20) Paine, T. K.; Weyhermüller, T.; Slep, L. D.; Neese, F.; Bill, E.; Bothe, E.; Wieghardt, K.; Chaudhuri, P. *Inorg. Chem.* **2004**, *43*, 7324−7338.

(21) (a) Morgenstern, B.; Steinhauser, S.; Hegetschweiler, K.; Garribba, E.; Micera, G.; Sanna, D.; Nagy, L. *Inorg. Chem.* **2004**, *43*, 3116−3126. (b) Morgenstern, B.; Kutzky, B.; Neis, C.; Stucky, S.; Hegetschweiler, K.; Garribba, E.; Micera, G. *Inorg. Chem.* **2007**, *46*, 3903−3915.

(22) Diamantis, A.; Manikas, M.; Salam, M.; Snow, M.; Tiekink, E. *Aust. J. Chem.* **1988**, *41*, 453−468.

(23) Raymond, K. N.; Isied, S. S.; Brown, L. D.; Fronczek, F. R.; Nibert, J. H. *J. Am. Chem. Soc.* **1976**, *98*, 1767−1774.

(24) (a) Karpishin, T. B.; Dewey, T. M.; Raymond, K. N. *J. Am. Chem. Soc.* **1993**, *115*, 1842−1851. (b) Micera, G.; Sanna, D. *Spectroscopic methods for the characterization of vanadium complexes*; Wiley: New York, 1998.

(25) Desideri, A.; Raynor, J. B.; Diamantis, A. A. *J. Chem. Soc., Dalton Trans.* **1978**, 423−426.

(26) Nagypál, I.; Fábián, I. *Inorg. Chim. Acta* **1982**, *61*, 109−113.

(27) Gran, G. *Acta Chem. Scand.* **1950**, *4*, 559−577.

(28) Irving, H. M.; Miles, M. G.; Pettit, L. D. *Anal. Chim. Acta* **1967**, *38*, 475−488.

(29) Gans, P.; Sabatini, A.; Vacca, A. *J. Chem. Soc., Dalton Trans.* **1985**, 1195−1200.

(30) Gans, P.; Sabatini, A.; Vacca, A. *Talanta* **1996**, 1739−1753.

(31) Henry, R. P.; Mitchell, P. C. H.; Prue, J. E. *J. Chem. Soc., Dalton Trans.* **1973**, 1156−1159.

(32) Davies, C. W. *J. Chem. Soc.* **1938**, 2093−2098.

(33) (a) Komura, A.; Hayashi, M.; Imanaga, H. *Bull. Chem. Soc. Jpn.* **1977**, *50*, 2927−2931. (b) Vilas Boas, L. F.; Costa Pessoa, J. In *Comprehensive Coordination Chemistry*; Wilkinson, G., Gillard, R. D., McCleverty, J. A., Eds.; Pergamon Press: Oxford, 1985; Vol. 3, pp 453−583.
(34) Zékány, L.; Nagypál, I. In *Computation Methods for the Determination of Formation Constants*; Leggett, D. J., Ed.; Plenum Press: New York, 1985; pp 291−353.
(35) *WINEPR SimFonia*, version 1.25; Bruker Analytische Messtechnik GmbH: Karlshrue, Germany, 1996.
(36) Frisch, M. J.; Trucks, G. W.; Schlegel, H. B.; Scuseria, G. E.; Robb, M. A.; Cheeseman, J. R.; Scalmani, G.; Barone, V.; Mennucci, B.; Petersson, G. A.; Nakatsuji, H.; Caricato, M. L.; Hratchian, H. P.; Izmaylov, A. F.; Bloino, J.; Zheng, G.; Sonnenberg, J. L.; Hada, M.; Ehara, M.; Toyota, K.; Fukuda, R.; Hasegawa, J.; Ishida, M.; Nakajima, T.; Honda, Y.; Kitao, O.; Nakai, H.; Vreven, T.; Montgomery, J. A., Jr.; Peralta, J. E.; Ogliaro, F.; Bearpark, M.; Heyd, J. J.; Brothers, E.; Kudin, K. N.; Staroverov, V. N.; Keith, T.; Kobayashi, R.; Normand, J.; Raghavachari, K.; Rendell, A.; Burant, J. C.; Iyengar, S. S.; Tomasi, J.; Cossi, M.; Rega, N.; Millam, J. M.; Klene, M.; Knox, J. E.; Cross, J. B.; Bakken, V.; Adamo, C. J.; Gomperts, R.; Stratmann, R. E.; Yazyev, O.; Austin, A. J.; Cammi, R.; Pomelli, C.; Ochterski, J. W.; Martin, R. L.; Morokuma, K.; Zakrzewski, V. G.; Voth, G. A.; Salvador, P.; Dannenberg, J. J.; Dapprich, S.; Daniels, A. D.; Farkas, Ö.; Foresman, J. B.; Ortiz, J. V.; Cioslowski, J.; Fox, D. J. In *Gaussian 09, revision C.01*; Gaussian, Inc.: Wallingford, CT, 2009.
(37) (a) Becke, A. D. *J. Chem. Phys.* **1993**, *98*, 5648−5652. (b) Perdew, J. P. *Phys. Rev. B* **1986**, *33*, 8822−8824.
(38) Krishnan, R.; Binkley, J. S.; Seeger, R.; Pople, J. A. *J. Chem. Phys.* **1980**, *72*, 650−654.
(39) (a) Bühl, M.; Kabrede, H. *J. Chem. Theory Comput.* **2006**, *2*, 1282−1290. (b) Bühl, M.; Reimann, C.; Pantazis, D. A.; Bredow, T.; Neese, F. *J. Chem. Theory Comput.* **2008**, *4*, 1449−1459.
(40) Micera, G.; Garribba, E. *Int. J. Quantum Chem.* **2012**, *112*, 2486−2498.
(41) (a) Perdew, J. P.; Burke, K.; Ernzerhof, M. *Phys. Rev. Lett.* **1996**, *77*, 3865−3868. (b) Perdew, J. P.; Burke, K.; Ernzerhof, M. *Phys. Rev. Lett.* **1997**, *78*, 1396−1396.
(42) Neese, F. In *ORCA - An Ab Initio, DFT and Semiempirical Program Package*, version 2.9; Max-Planck-Institute for Bioinorganic Chemistry: Mülheim a. d. Ruhr, Germany, 2012.
(43) (a) Micera, G.; Garribba, E. *Dalton Trans.* **2009**, 1914−1918. (b) Micera, G.; Pecoraro, V. L.; Garribba, E. *Inorg. Chem.* **2009**, *48*, 5790−5796. (c) Gorelsky, S.; Micera, G.; Garribba, E. *Chem.—Eur. J.* **2010**, *16*, 8167−8180. (d) Micera, G.; Garribba, E. *Eur. J. Inorg. Chem.* **2010**, 4697−4710. (e) Lodyga-Chruscinska, E.; Micera, G.; Garribba, E. *Inorg. Chem.* **2011**, *50*, 883−899. (f) Micera, G.; Garribba, E. *J. Comput. Chem.* **2011**, *32*, 2822−2835. (g) Micera, G.; Garribba, E. *Eur. J. Inorg. Chem.* **2011**, 3768−3780. (h) Sanna, D.; Pecoraro, V.; Micera, G.; Garribba, E. *J. Biol. Inorg. Chem.* **2012**, *17*, 773−790.
(44) (a) Miertuš, S.; Scrocco, E.; Tomasi, J. *Chem. Phys.* **1981**, *55*, 117−129. (b) Miertuš, S.; Tomasi, J. *Chem. Phys.* **1982**, *65*, 239−245. (c) Cossi, M.; Barone, V.; Cammi, R.; Tomasi, J. *Chem. Phys. Lett.* **1996**, *255*, 327−335.
(45) Marenich, A. V.; Cramer, C. J.; Truhlar, D. G. *J. Phys. Chem. B* **2009**, *113*, 6378−6396.
(46) (a) Lodyga-Chruscinska, E.; Sanna, D.; Garribba, E.; Micera, G. *Dalton Trans.* **2008**, 4903−4916. (b) Sanna, D.; Buglyó, P.; Bíró, L.; Micera, G.; Garribba, E. *Eur. J. Inorg. Chem.* **2012**, 1079−1092.
(47) (a) Lindstrom, F.; Diehl, H. *Anal. Chem.* **1960**, *32*, 1123−1127. (b) Vytřas, K.; Kalous, J.; Černá-Frýbortová, J. *Talanta* **1990**, *37*, 1025−1027. (c) Kratochvil, B.; Nolan, J.; Cantwell, F. F.; Fulton, R. B. *Can. J. Chem.* **1981**, *59*, 2539−2542.
(48) (a) Bigoli, F.; Leporati, E.; Pellinghelli, M. *Ann. Chim. (Rome, Italy)* **1983**, *73*, 481−493. (b) Sarin, R.; Munshi, K. *J. Indian Chem. Soc.* **1978**, *55*, 512−513.
(49) Kosak, A.; Ballczo, W. *Fresenius' J. Anal. Chem.* **1971**, *253*, 188−191.
(50) (a) Chasteen, D. N. In *Biological Magnetic Resonance*; Berliner, L. J. J., Reuben, J., Eds.; Plenum Press: New York, 1981; Vol. 3, pp 53−119. (b) Smith, T. S., II; LoBrutto, R.; Pecoraro, V. L. *Coord. Chem. Rev.* **2002**, *228*, 1−18.
(51) Pisano, L.; Varnagy, K.; Timári, S.; Hegetschweiler, K.; Micera, G.; Garribba, E. *Inorg. Chem.* **2013**, *52*, 5260−5272.
(52) Castiñeiras Campos, A.; Silica Zafra, A. G.; González Pérez, J. M.; Niclós Gutiérrez, J.; Chinea, E.; Mederos, A. *Inorg. Chim. Acta* **1996**, *241*, 39−45.
(53) Weyhermüller, T.; Paine, T. K.; Bothe, E.; Bill, E.; Chaudhuri, P. *Inorg. Chim. Acta* **2002**, *337*, 344−356.
(54) Steinhauser, S.; Heinz, U.; Bartholomä, M.; Weyhermüller, T.; Nick, H.; Hegetschweiler, K. *Eur. J. Inorg. Chem.* **2004**, 4177−4192.
(55) Steinhauser, S.; Heinz, U.; Sander, J.; Hegetschweiler, K. *Z. Anorg. Allg. Chem.* **2004**, *630*, 1829−1838.
(56) (a) Ito, S.; Sato, Y.; Mizuguchi, J. *Acta Crystallogr., Sect. E* **2008**, *64*, m333−m334. (b) Koley, M. K.; Sivasubramanian, S. C.; Varghese, B.; Manoharan, P. T.; Koley, A. P. *Inorg. Chim. Acta* **2008**, *361*, 1485−1495.
(57) (a) Mizuguchi, J.; Uta, K.; Sato, Y. *Acta Crystallogr., Sect. E* **2007**, *63*, m1329−m1330. (b) Travnicek, Z.; Sindelar, Z.; Marek, J. *Z. Kristallogr. − New Cryst. Struct.* **1997**, *212*, 125−126.
(58) Hefele, H.; Ludwig, E.; Uhlemann, E.; Weller, F. *Z. Anorg. Allg. Chem.* **1995**, *621*, 1973−1976.
(59) Dutta, S.; Basu, P.; Chakravorty, A. *Inorg. Chem.* **1993**, *32*, 5343−5348.
(60) Dutta, S.; Basu, P.; Chakravorty, A. *Inorg. Chem.* **1991**, *30*, 4031−4037.
(61) Owiny, D.; Parkin, S.; Ladipo, F. T. *J. Organomet. Chem.* **2003**, *678*, 134−141.
(62) Yang, L. L.; Dang, Z. H.; Xu, L. *Chin. J. Struct. Chem.* **2009**, *28*, 493−497.
(63) Sawusch, S.; Schilde, U.; Uhlemann, E. *Z. Naturforsch., B: Chem. Sci.* **1997**, *52*, 61−64.
(64) Labisbal, E.; Rodríguez, L.; Vizoso, A.; Alonso, M.; Romero, J.; García-Vázquez, J.-A.; Sousa-Pedrares, A.; Sousa, A. *Z. Anorg. Allg. Chem.* **2005**, *631*, 2107−2114.
(65) Favas, M. C.; Kepert, D. L. *J. Chem. Soc., Dalton Trans.* **1978**, 793−797.
(66) Sanna, D.; Varnágy, K.; Timári, S.; Micera, G.; Garribba, E. *Inorg. Chem.* **2011**, *50*, 10328−10341.
(67) Farahbakhsh, M.; Nekola, H.; Schmidt, H.; Rehder, D. *Chem. Ber.* **1997**, *130*, 1129−1133.
(68) Sanna, D.; Ugone, V.; Micera, G.; Garribba, E. *Dalton Trans.* **2012**, *41*, 7304−7318.
(69) Rangel, M.; Leite, A.; João Amorim, M.; Garribba, E.; Micera, G.; Lodyga-Chruscinska, E. *Inorg. Chem.* **2006**, *45*, 8086−8097.
(70) Gillard, D. R.; Lancashire, J. R. *Phytochemistry* **1984**, *23*, 179−180.
(71) Ballhausen, C. J.; Gray, H. B. *Inorg. Chem.* **1962**, *1*, 111−122.
(72) Garribba, E.; Micera, G.; Sanna, D. *Inorg. Chim. Acta* **2006**, *359*, 4470−4476.
(73) Mabbs, F. E.; Collison, D. *Electron Paramagnetic Resonance of d Transition Metal Compounds*; Elsevier Science Publishers B.V.: Amsterdam, 1992.
(74) Smith, T. S.; Root, C. A.; Kampf, J. W.; Rasmussen, P. G.; Pecoraro, V. L. *J. Am. Chem. Soc.* **2000**, *122*, 767−775.

NOTE ADDED AFTER ASAP PUBLICATION

Due to a production error, this paper was published on the Web on July 2, 2013, with errors in Tables 1 and 3, and minor text errors. The corrected version was reposted on July 3, 2013.